SPECTRAL CHARACTERISTICS OF VLF EMISSIONS OBSERVED BY B_{15}-4N BALLOON LAUNCHED FROM ESRANGE IN SWEDEN

Takayuki ONO, Hiroshi MIYAOKA and Masaki EJIRI

National Institute of Polar Research, 9–10, Kaga 1-chome, Itabashi-ku, Tokyo 173

Abstract: A high-sensitive VLF wave observation has been carried out using the stratospheric balloon (B_{15}-4N) launched from Esrange in Sweden on December 9, 1982. The VLF receiving system installed on the balloon has been equipped with a large one-turn loop antenna attached along the balloon surface. During the level flight at an altitude of 30 km, power line harmonic radiations and periodic emissions with the repetition period of about 2.7 s have been observed in connection with the development of an auroral substorm. In this paper, spectral characteristics of these emissions are examined based on the dynamic spectral analysis in order to clarify the feature of the wave-particle interactions relating to the generation of these emissions.

1. Introduction

The National Institute of Polar Research has made a balloon experiment at Esrange, Sweden coordinated with ground support observations during the period from November 3 to December 21, 1982. This campaign was organized and performed as an international balloon campaign named SAMBO-82 (Simultaneous Auroral Multi-Balloon Observation) in cooperation with the following institutes; SSC (Swedish Space Corporation), KGI (Kiruna Geophysical Institute), TUG (Technical University, Graz) and PGI (Polar Geophysical Institute, Murmansk). In this campaign, two sets of the balloon payload, B_{15}-2N and B_{15}-4N, have been prepared by our institute. The B_{15}-2N payload was provided with the instruments for auroral X-ray, electric fields and ELF-VLF waves, whereas the B_{15}-4N had instruments for visible aurora image, auroral X-ray image, and electromagnetic waves in the VLF-MF frequency range. One of the most significant aims of these balloon experiments was to seek for the relationship between the spatial distribution of auroral particle precipitation and related VLF wave phenomena, *e.g.*, auroral hiss and chorus emissions. There have been observed many evidences indicating the close correlation between the occurrence of VLF emissions and the particle precipitations in the polar ionosphere. Particularly, X-ray microbursts have been investigated in detail comparing them with chorus type VLF emissions observed by satellites (*e.g.*, OLIVEN and GURNETT, 1968) and balloons (ROSENBERG *et al.*, 1971, 1978). We also took up these phenomena as a main subject in this balloon experiment. The B_{15}-4N balloon was launched twice successfully on November 25 and December 9, 1982. In the second flight, there were observed remarkable periodic VLF emissions and power line harmonic radiations

using a newly developed high-sensitive VLF receiving system with a large one-turn loop antenna. In this paper, we present several prominent features of dynamic spectra of these emissions and discuss the generation mechanism of these wave phenomena.

2. Instrumentation

The most significant characteristics of the VLF receiving system on board the

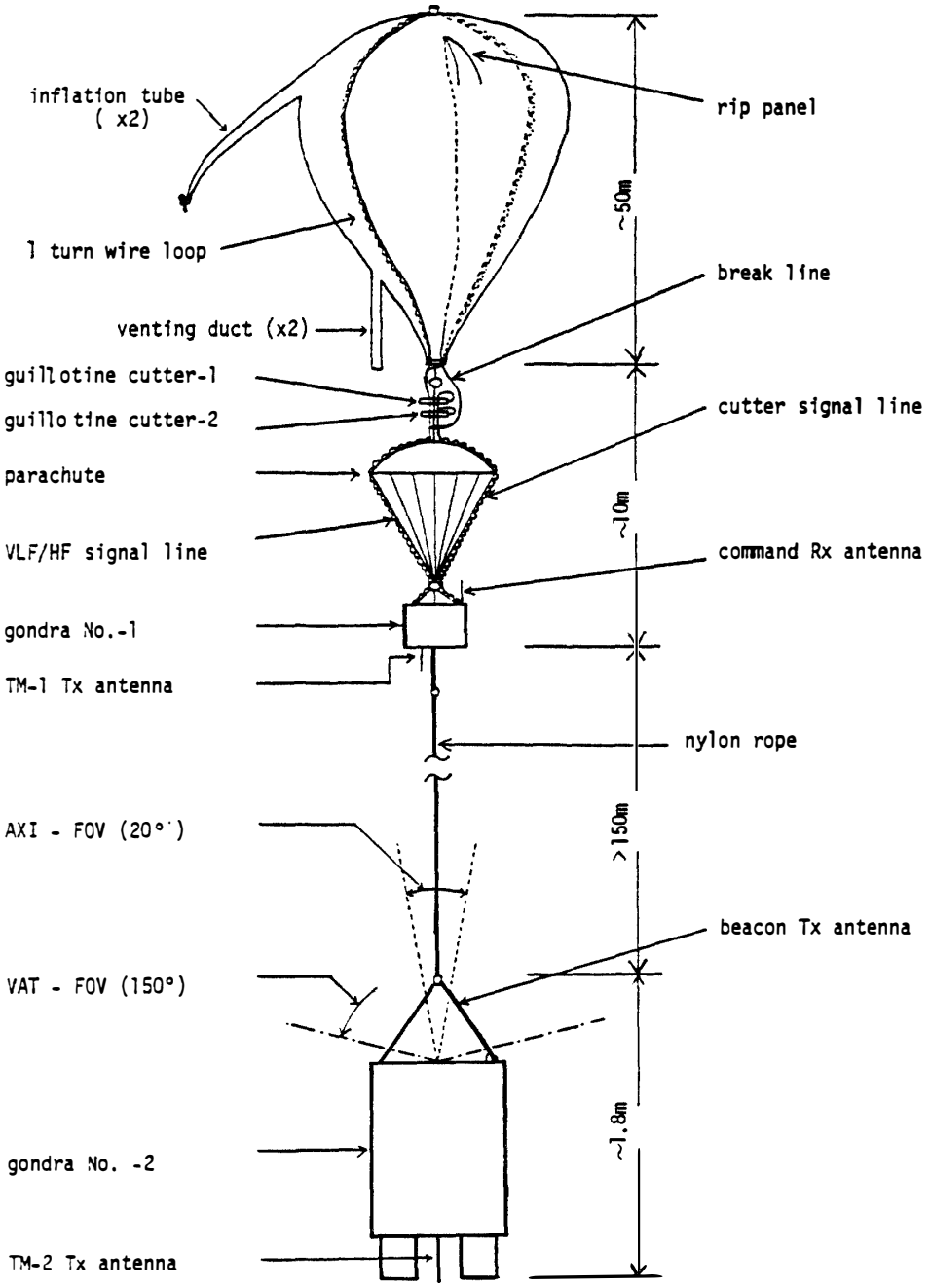

Fig. 1. Flight train of the B_{15}-4N balloon. A one-turn loop antenna is extented around the balloon surface.

B_{15}-4N payload is the loop antenna extended along the balloon surface. As shown in Fig. 1, the copper wire with a diameter of 1.45 mm is attached along the surface of the balloon meridian. The balloon with a volume of 14700 m^3 is 102.7 m in circumference and has a meridian section area of 696 m^2. This wide open area of the loop antenna made it possible to serve as a high sensitive VLF receiver since the effective height (h_{eff}) of the one-turn loop antenna is proportional to the area as

$$h_{eff}=S\cdot k\,, \tag{1}$$

where S and k are the open area of a loop antenna, and the wavenumber of the VLF wave, respectively. The resistance (R_a) and the reactance (L_a) of the loop antenna are 1.46 ohms and 184 microhenry, respectively. When the resistance of the feeder cable line (R_f) and the input impedance of the receiver (Z_i) are known, we can calculate the input signal level into the receiver (V) for the field strength of the VLF signal (E), as

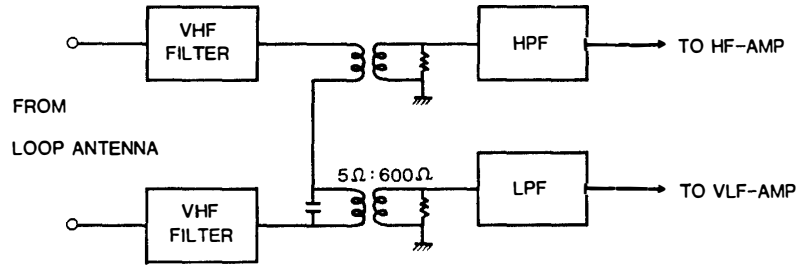

Fig. 2. Divider circuit for VLF and HF waves detected by the loop antenna.

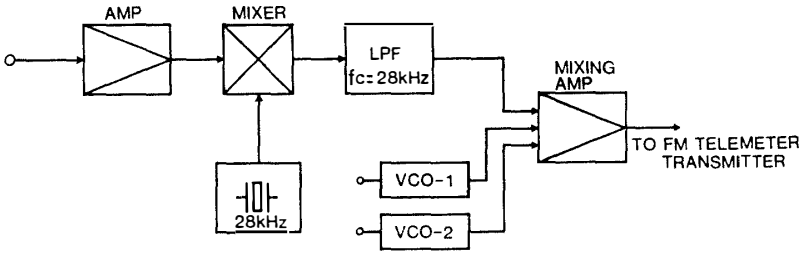

Fig. 3. Modulation circuit of VLF waves for the telemeter transmitter.

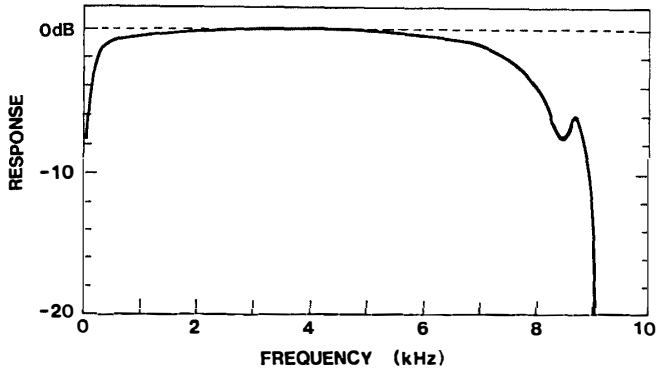

Fig. 4. Over-all frequency response of the VLF receiver on board the B_{15}-4N balloon.

$$V=\frac{Z_i}{R_a+j\cdot L_a+R_f+Z_i}k\cdot S\cdot E\,, \tag{2}$$

where $(j)^2=-1$.

As has been given in Fig. 2, a detected signal in the VLF range is selected by the divider circuit, and fed into the VLF amplifier. Special filtering circuits are used in the divider circuit, one is a VHF filter to reject the strong telemeter signal in the VHF range, the other is a low pass filter to cut off the strong omega signal in the frequency range from 10.24 to 13.6 kHz. The block diagram of the VLF amplifier and modulation circuit for the telemeter transmitter is shown in Fig. 3. The VLF signal is amplified by the low noise amplifier and modulated by an LSB modulation circuit with a center frequency of 28 kHz. The LSB modulation signal is added with two FM subcarrier signals used for other instruments, then supplied into the FM telemeter transmitter with the carrier frequency of 245.88 MHz. The overall frequency characteristics of the VLF receiver are shown in Fig. 4.

Finally, using the relationship between the field strength (E; V/m$\cdot\sqrt{\text{Hz}}$) and the power flux density as,

$$P=\frac{E^2}{376.7}\,, \tag{3}$$

the equivalent power flux density is estimated to be about 2.14×10^{-16} W/m^{2}Hz at 3.5 kHz for the output noise level of the VLF receiver.

3. Observation

The second flight of the B_{15}-4N balloon has started at 1722 UT and ended at 2145 UT on December 9, 1982. The balloon reached the ceiling level of 30 km at about 2020 UT. From a viewpoint of the sensitivity of the VLF receiver, an effective signal reception is supposed to start at about 19 UT. Due to the 15% lifting force of the balloon, the atmospheric pressure level where the open area of the loop antenna becomes a half value, can be roughly estimated as,

$$P=P_0\times(1+0.15)\times2^{1.5}\,, \tag{4}$$

where P_0 is the atmospheric pressure at the ceiling level. The altitude for the pressure P is about 23 km, *i.e.*, about 19 UT of the flight time.

Figure 5 gives the successive display of dynamic spectra of the VLF waves received during the whole flight of the B_{15}-4N balloon. In Fig. 5, the power line noise was affected by the electrical equipment near the launching area and rapidly disappeared except the third harmonic noise. After 1730 UT, the dynamic spectrum displays only atmospherics, the third harmonic of power line radiation, and weak interference noise line of 3.8 kHz. The spectrum of the atmospherics in the frequency band from 6 to 8 kHz shows the intensifying and spreading feature. This feature indicates the increased sensitivity of the loop antenna with the altitude of the balloon. The reception of VLF waves with the maximum sensitivity continues during the period after 2000 UT. The natural VLF emissions occur in the following three frequency bands; i) ELF band below 1 kHz, ii) VLF band from 2.5 to 5 kHz and iii) VLF band

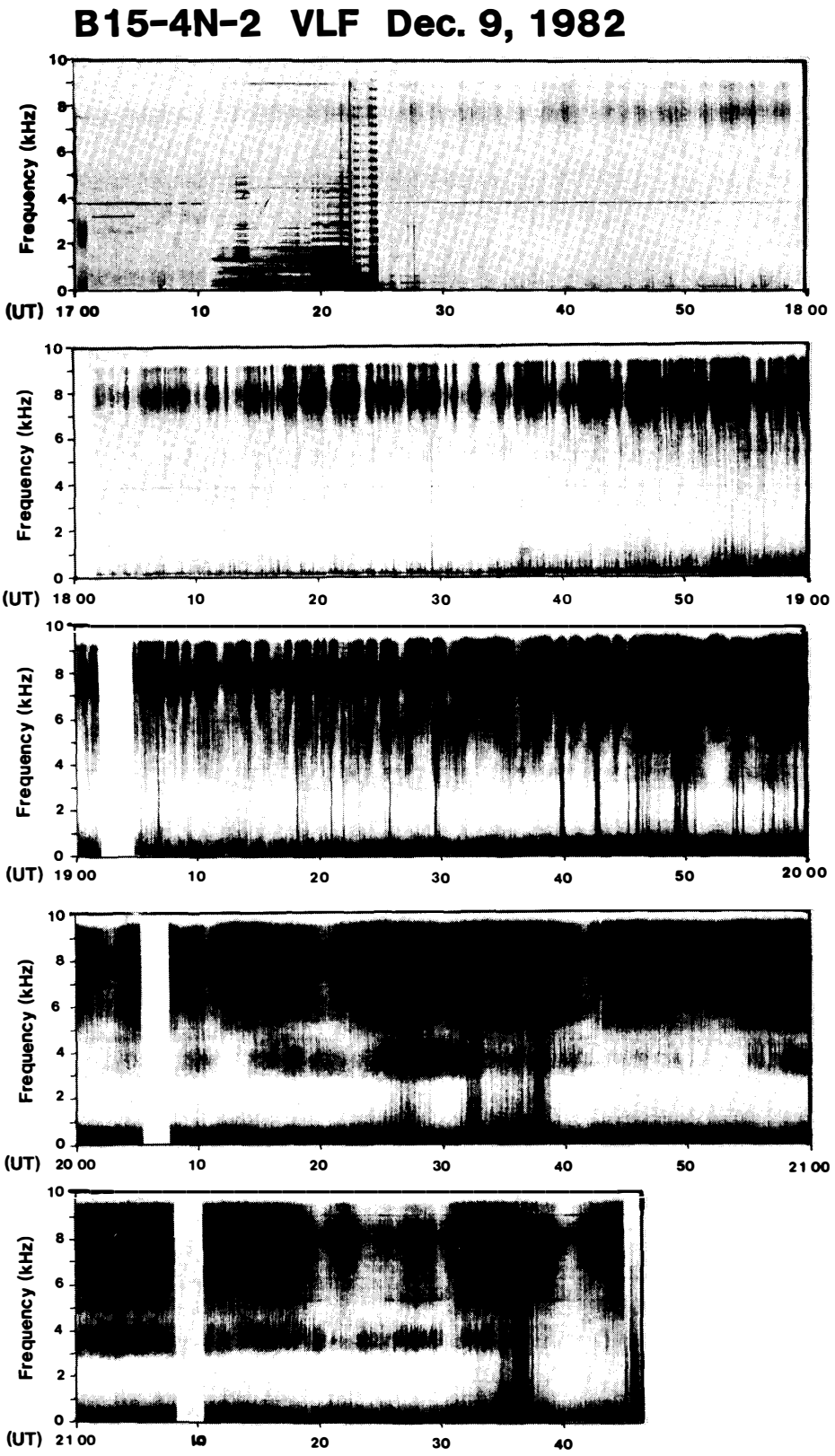

Fig. 5. Dynamic (f-t) spectra of VLF waves in the frequency range below 10 kHz detected by the VLF receiver on board the B_{15}-4N balloon on December 9, 1982.

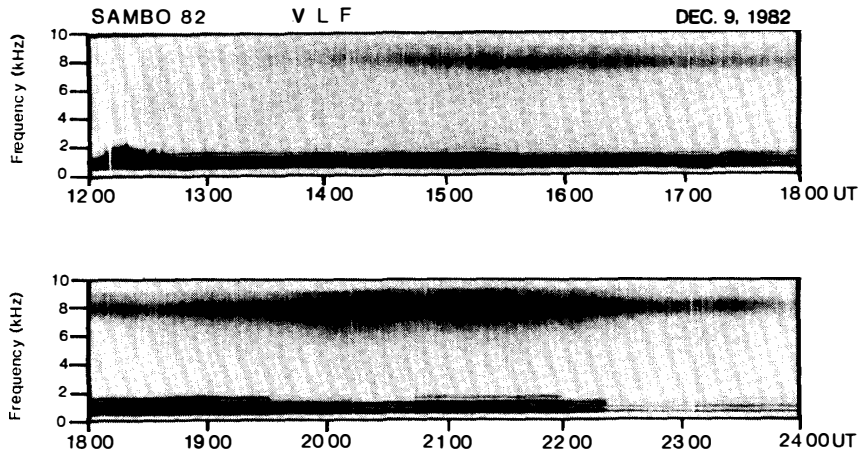

Fig. 6. Dynamic (f-t) spectra of VLF waves observed on the ground at Esrange. VLF hiss emissions are intensified around 8 kHz in the period of 2000–2200 UT.

above 5 kHz.

The emission band i includes atmospherics, and power line harmonic radiations. The emission band iii also consists of atmospherics, and partially may include VLF hiss emission, because the activity of VLF hiss emissions was enhanced at the same time on the ground, as shown in the dynamic spectrum of VLF waves observed at Esrange (Fig. 6).

In the intermediate emission band ii, there can be seen an obvious emission coming from the upper ionosphere. The power of the emission is very weak, so it was scarcely found in the ground observation data. Figures 7 and 8 show the power flux of the emission bands ii and iii, respectively. The power flux at 8 kHz (band iii) is in the range from 10^{-13} to 10^{-12} W/m^2 Hz, and presents a spin modulation caused by the directional sensitivity of the loop antenna due to the balloon rotation. The power

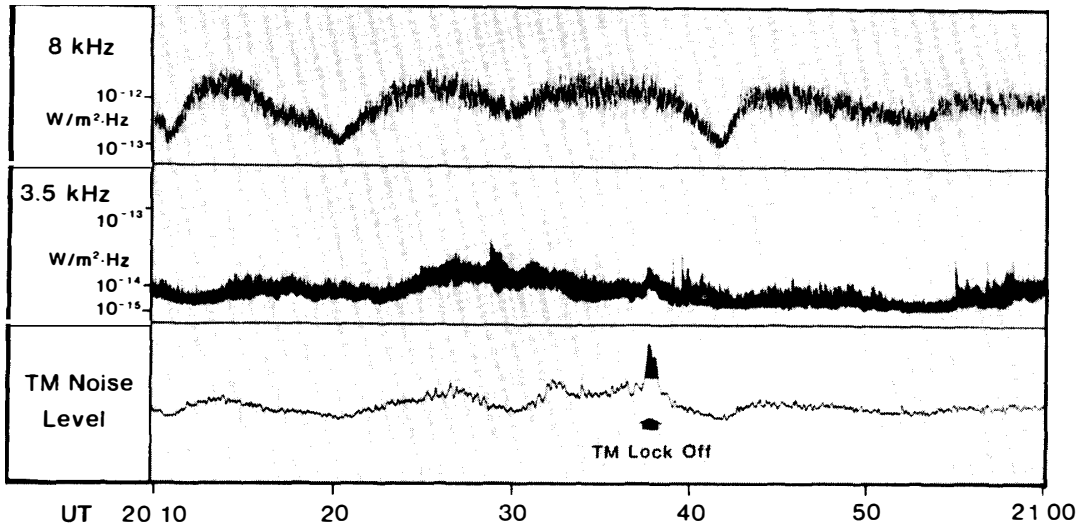

Fig. 7. Power flux of VLF waves at the frequencies of 8 and 3.5 kHz, and the telemeter noise level in the interval of 2010–2100 UT. Enhancement of the noise level at about 2038 UT is caused by the telemeter lock-off.

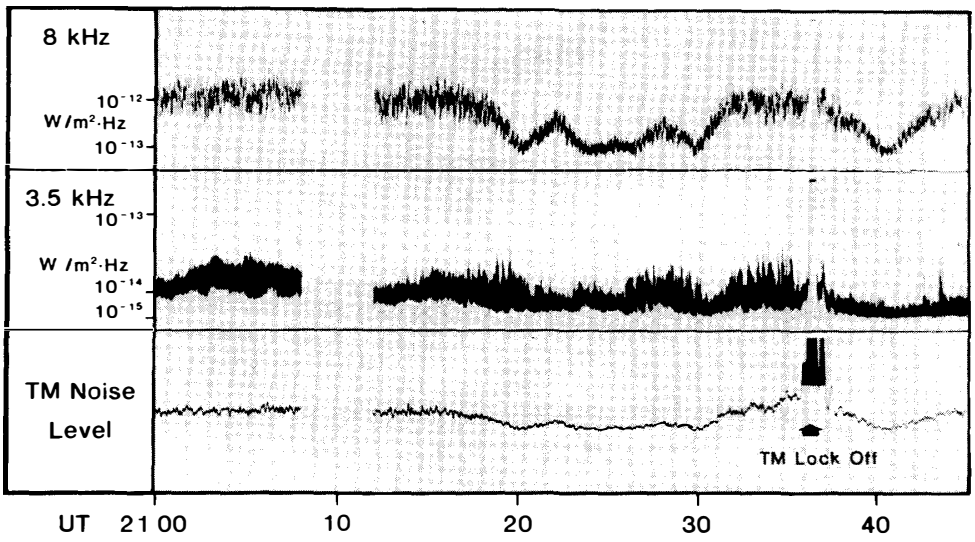

Fig. 8. Same as Fig. 7 except for the interval of 2100–2145 UT.

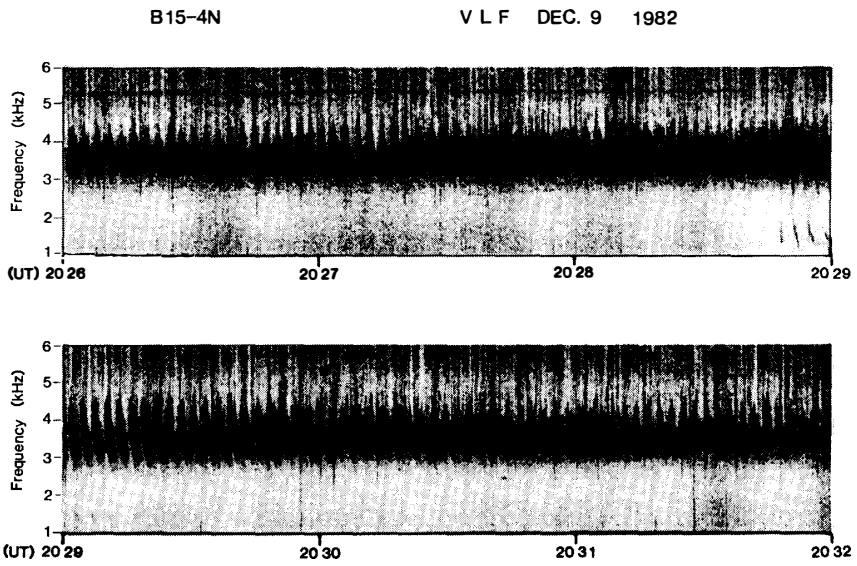

Fig. 9. Expanded dynamic (f-t) spectrum of VLF emissions observed by the B_{15}-4N flight during 2026–2032 UT. Periodic emissions with a repetition period of about 2.7 s are clearly observed in the frequency range of 3–4.5 kHz.

flux at 3.5 kHz shows the successive impulses in the range of 10^{-15}–5×10^{-14} W/m²Hz, and there is no modulation due to the balloon rotation. So, it is considered that band ii emission came from the zenith of the balloon, whereas the main part of the band iii emission arrived from the horizon with a rather narrow view angle of the direction.

We can see the four types of prominent spectral feature in the band ii emission by a detailed spectrum analysis.

1) As indicated in Fig. 9, periodic emissions repeating with a regular periodicity of about 2.7 s tend to form a falling tone structure. This emission is sometimes triggered by whistlers as shown at about 2028: 50 UT.

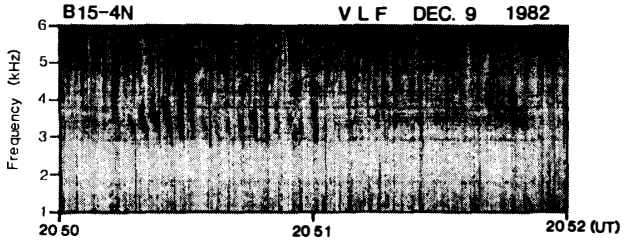

Fig. 10. Same as Fig. 9 except for the interval of 2050–2052 UT. Power line harmonic emissions are observed in the period of 2051–2052 UT.

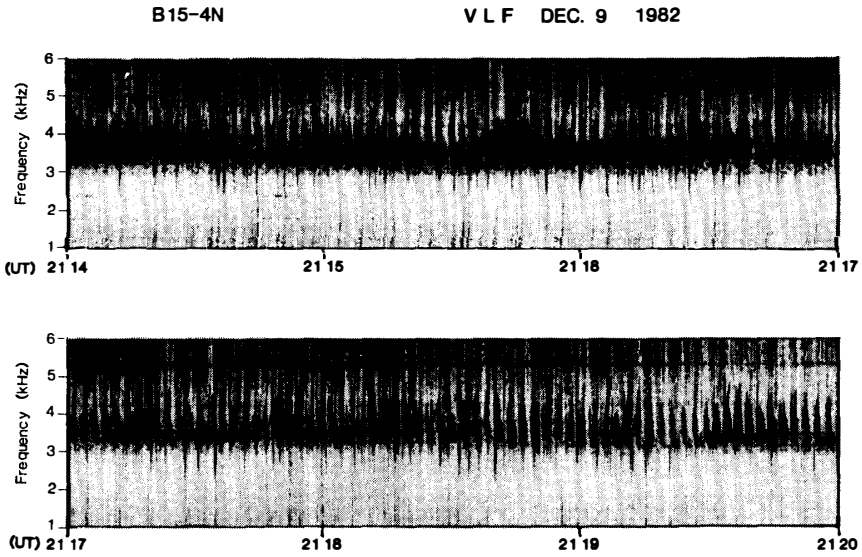

Fig. 11. Same as Fig. 10 except for the time interval of 2114–2120 UT. Quasi-periodic modulation of the periodic emissions is found in the period of 2117–2120 UT.

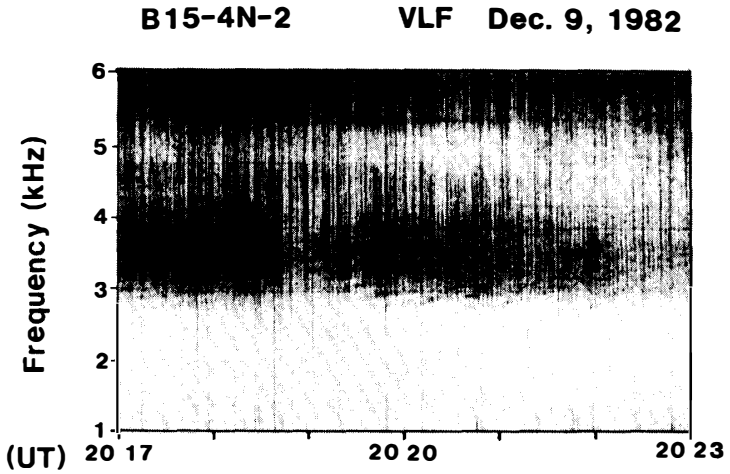

Fig. 12. Dynamic (f-t) spectrum of the periodic emissions in the period of 2017–2023 UT. A feature of long-term frequency drift is clearly identified.

2) In Fig. 10, power line harmonic radiations are found clearly in the period from 2051 UT to 2052 UT. The odd harmonic frequency of 50 Hz is dominant in

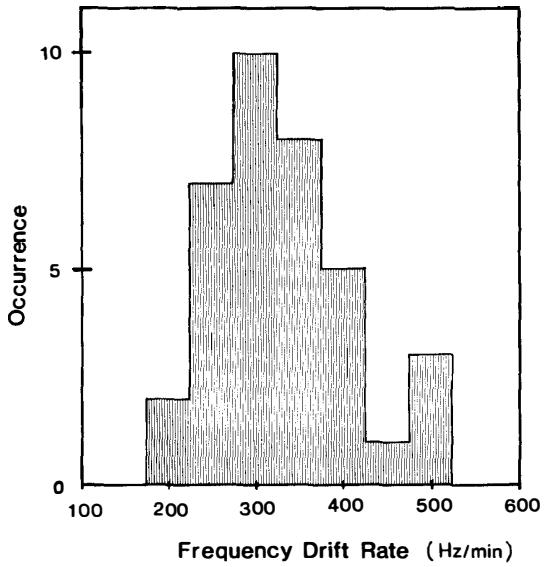

Fig. 13. Occurrence of the frequency drift rate caused by the quasi-periodic modulation observed in the time interval of 2010–2040 UT.

this emission. The emission appeared only in the range from 2.5 to 4.5 kHz, the same range as the other natural emissions. It is expected therefore, that the emission is amplified in the magnetosphere.

3) In Fig. 11, emissions are triggered by power line harmonic emissions. Such a triggering feature can be seen clearly at 2119: 30 UT. It is interesting, furthermore, that the preceding falling tone of the periodic emission faded at the triggering frequency. In most cases the triggering frequency lies in the range from 3 to 4 kHz.

4) When we select another time scale for a display, a new spectral feature can be seen in the dynamic spectrum. As shown in Fig. 12, a long-term rising tone can be seen during the period from 2017: 26 to 2020: 12 UT, with the frequency changing from 2.7 to 3.0 kHz. The drift rate of this rising tone is found to be in the range of 200–500 Hz/min, with the peak occurring at about 300 Hz/min, as shown in Fig. 13.

4. Discussion

According to *Kp* index on December 9, 1982, the magnetic activity was rather moderate during the flight time of the balloon. The *Kp* index showed the maximum value of 5^+ at about 15 UT, then the *Kp* decreased to 3^- when the balloon reached the ceiling altitude of the flight. The magnetic variations observed at Esrange indicate that magnetic disturbances occurred twice on December 9 as shown in Fig. 14. However, it seems that CNA data show no significant absorptions. The first event of the positive magnetic variation started around 13 UT, and the second negative event started around 20 UT. As has already seen in Fig. 6, the ground VLF observation indicates that an enhancement of hiss emissions around 8 kHz started around 14 UT and continued to 24 UT. Thus, we can conclude that the VLF waves observed by the B_{15}-4N balloon contain VLF hiss emission, although it suffered from intense atmospheric noise pulses.

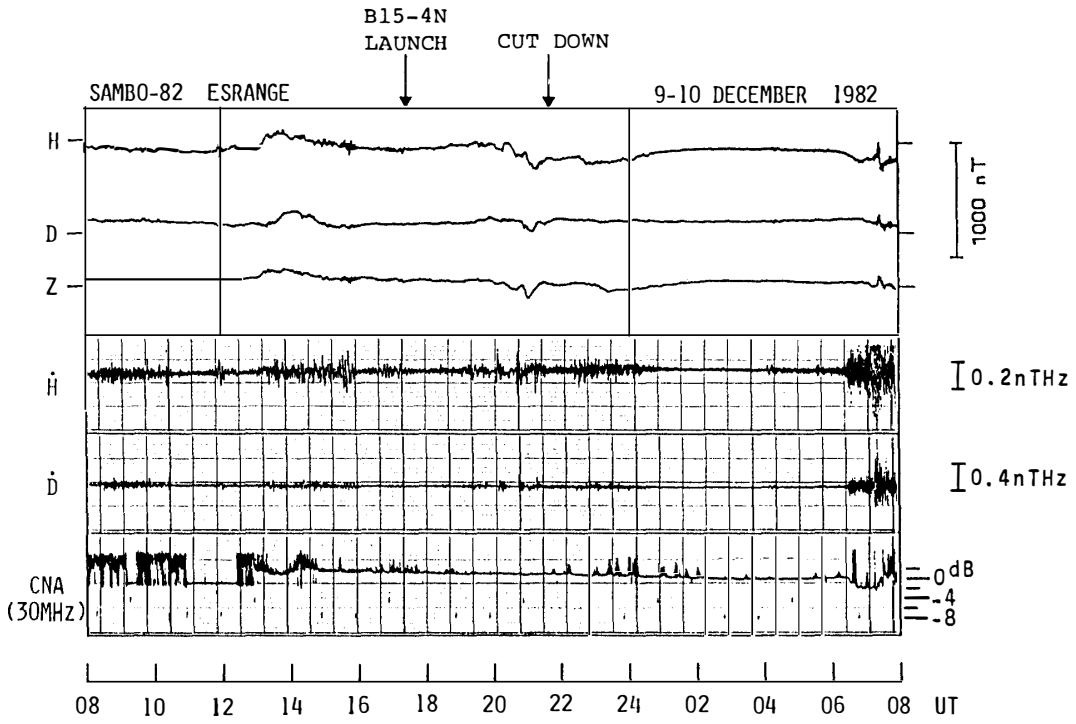

Fig. 14. Summary plot of the geomagnetic activity on December 9–10, 1982. It contains geomagnetic field variations (3 components), ULF pulsations (2 components) and the cosmic noise absorption at 30 MHz. The launching and cut-down times are indicated by arrows.

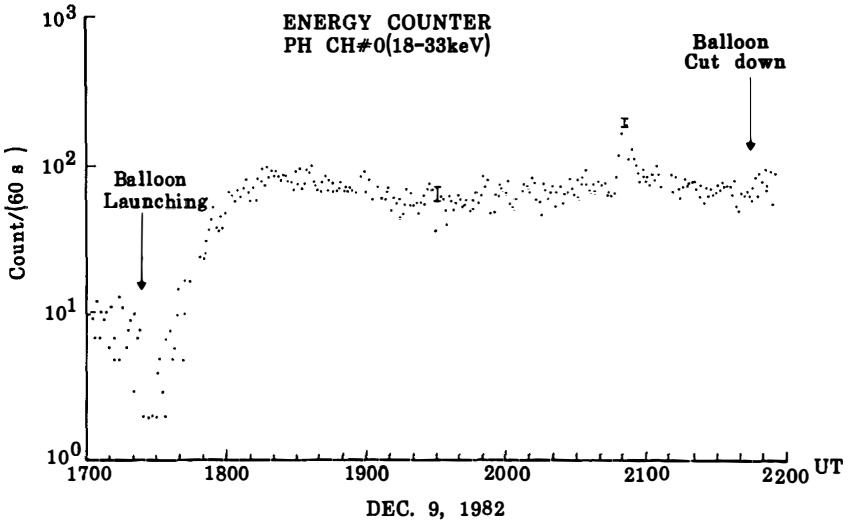

Fig. 15. Auroral X-ray data observed by the X-ray detector on board the same balloon. A weak event of X-ray burst is observed at about 2050 UT (after HIRASIMA et al., 1984).

The continuation of VLF hiss reception on the ground from 20 to 22 UT means that precipitation of high energy particle is absent in the zenith of Esrange, as has been confirmed by the CNA data in Fig. 14. This fact is further confirmed by the X-ray observation on board the same balloon (HIRASIMA *et al.*, 1984). In Fig. 15, a weak X-ray event can be found around 2050 UT, the same time as the magnetic dis-

turbance presented in Fig. 14. The enhancement of X-ray appeared only in the energy range below 60 keV. It is considered, therefore, that no effective absorption occurred at Esrange and the balloon observation points.

The spin modulation of the power flux at 8 kHz in Figs. 7 and 8 can be recognized that a main part of the observed power flux is atmospherics noises. There was a big snowstorm in the North Sea, southwest of Esrange on December 9, so that strong atmospherics might occur near the center of the storm.

The most significant VLF emissions in the intermediate frequency band are thought to be stimulated in the equator region of the magnetosphere, as it is well known that the magnetospheric plasma is closely correlated with the history of magnetic disturbances (CARPENTER, 1967; CHAPPELL *et al.*, 1970; CHAPPELL, 1972). As for the plasma condition during the balloon flight on December 9, it might be a rapidly growing phase of the plasma density in the plasmasphere just inside the plasmapause, following the strong magnetic disturbance which occurred around 13 UT. Therefore, a strong wave-particle interaction would take place near the plasmapause due to the encounter of the injected high energy electrons and the cold ambient plasma. The periodic emission and the power line harmonic radiation can be recognized as a result of the amplification of wave packets caused by the electron cyclotron interaction (BRICE, 1965; HELLIWELL *et al.*, 1975; PARK and HELLIWELL, 1978), whereas the triggered emissions (triggered by one of the power line harmonic radiations) are considered to be caused by the nonlinear wave-particle interactions between the two kinds of wave packets, *i.e.*, the periodic emission and the power line harmonic radiation. The main feature seems to be the same as the emissions reported by HELLIWELL and KATSUFRAKIS (1974) and KIMURA *et al.* (1981), which are triggered by the VLF transmitter signal emitted from Siple Station, Antarctica. The triggered emission in this case is, however, characterized by the selection of triggering wave among the multiple sources of harmonic frequencies separated by about 100 Hz. The long-term varia-

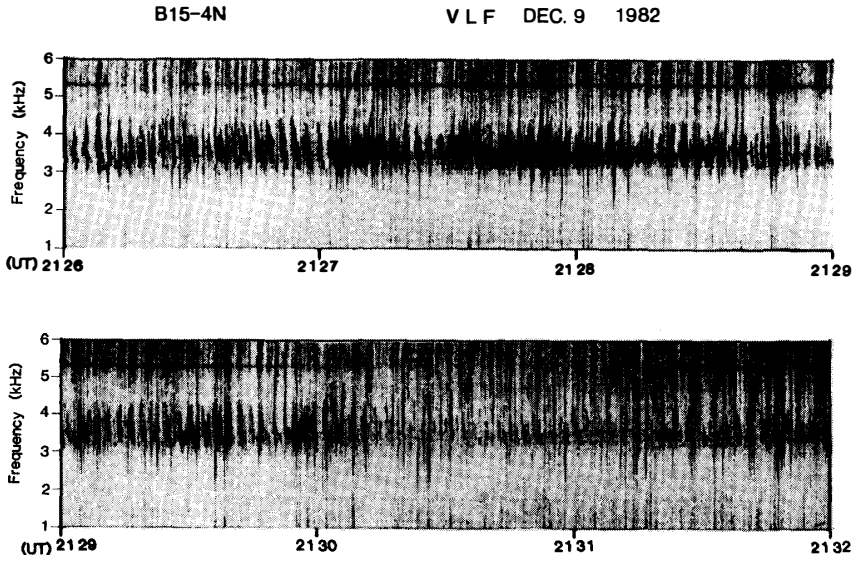

Fig. 16. Same as Fig. 9 except for the interval of 2126–2132 UT.

tion of the spectrum with the drift rate of about 300 Hz/min is different from slow spectral variations reported previously (SATO and KOKUBUN, 1980). One of the slow frequency drifts is associated with the quasi-periodic emission, the drift rate being an order of several kHz/min. Some repetitions of a quasi-periodic emission are found also in Fig. 16. During the periods from 2126 to 2127 UT and from 2129 to 2130 UT, frequencies with the maximum intensity of periodic emissions increased with a drift rate of about 3 kHz/min. Another feature of the frequency drift can be found in the long-term spectral variation of ELF chorus emissions. Sometimes, a dynamic spectrum of a cluster of chorus emissions presents a gradual rising tone feature (SATO *et al.*, 1983). This frequency drift rate is in the range of several hundred Hz/min, nearly the same as that in Fig. 13.

The mechanism causing the frequency drift is considered to have two candidates, *i.e.*, i) propagation of the region of the wave-particle interaction modulated by ULF compressional waves, and ii) change of the plasma conditions due to the plasma flow. When we assume the value of 300 Hz/min as a change of the electron cyclotron frequency in the source region of the emissions, we can convert the frequency drift rate into the displacement of the source region at the magnetospheric equator as a speed of about 10 km/s. This value is much lower than the propagation speed of ULF waves, but it is comparable to the convection speed of the magnetospheric plasma. The candidate ii) is, therefore, the possible mechanism of the frequency drift with the value of 300 Hz/min. However, it is still rather difficult to explain why the spectrum shows such a filamentary structure.

Acknowledgments

We express our thanks to Messrs. A. HELGER, B. SJÖHOLM and other staff members of Swedish Space Corporation at Esrange for their efforts in conducting this balloon campaign. We also thank Prof. J. NISHIMURA and his staff members at The Institute of Space and Astronautical Science, for their valuable guidance and usefull advices on the preparation of our balloon payloads and flight trains. This balloon experiment has been carried out as part of the SAMBO-82 international balloon campaign in cooperation with the following institutes; Kiruna Geophysical Institute (Dr. G. GUSTAVSSON), Polar Geophysical Institute (Dr. L. L. LAZUTIN) and Technical University, Graz (Prof. W. RIEDLER).

References

BRICE, N. (1965): Multiphase periodic very-low-frequency emission. Radio Sci., **69D**, 257–265.

CARPENTER, D. L. (1967): Relationship between the dawn minimum in the equatorial radius of the plasmapause and *Dst*, K_p, and local *K* at Byrd Station. J. Geophys. Res., **72**, 2969–2974.

CHAPPELL, C. R. (1972): Recent satellite measurements of the morphology and dynamics of the plasmasphere. Rev. Geophys. Space Phys., **10**, 951–979.

CHAPPELL, C. R., HARRIS, K. K. and SHARP, G. W. (1970): A study of the influence of magnetic activity on the location of the plasmapause as measured by OGO 5. J. Geophys. Res., **75**, 50–56.

HELLIWELL, R. A. and KATSUFRAKIS, J. P. (1974): VLF wave injection into the magnetosphere from

Siple Station, Antarctica. J. Geophys. Res., **79**, 2511–2518.

HELLIWELL, R. A., KATSUFRAKIS, J. P., BELL, T. F. and RAGHURAM, R. (1975): VLF line radiation in the earth's magnetosphere and its association with power system radiation. J. Geophys. Res., **80**, 4249–4258.

HIRASIMA, Y., MURAKAMI, H., OKUDAIRA, K., FUJII, M., NISHIMURA, J., YAMAGAMI, T., EJIRI, M., MIYAOKA, H., ONO, T. and KODAMA, M. (1984): Balloon observations of auroral X-rays at Esrange, Sweden and related phenomena. Mem. Natl Inst. Polar Res., Spec. Issue, **31**, 144–155.

KIMURA, I., MATSUMOTO, H., MUKAI, T., HASHIMOTO, K., HELLIWELL, R. A., BELL, T. F., INAN, U. S. and KATSUFRAKIS, J. R. (1981): Jikiken (EXOS-B) observation of Siple transmissions. Active Experiments in Space Plasmas, ed. by C. T. RUSSELL and M. J. RYCROFT. Oxford, Pergamon Press, 197–202 (Adv. Space Res., Vol. 1, No. 2).

OLIVEN, M. N. and GURNETT, D. A. (1968): Microburst phenomena, 3. An association between microbursts and VLF chorus. J. Geophys. Res., **73**, 2355–2362.

PARK, C. G. and HELLIWELL, R. A. (1978): Magnetospheric effect of powe line radiation. Science, **200**, 727–730.

ROSENBERG, T. J., HELLIWELL, R. A. and KATSUFRAKIS, J. P. (1971): Electron precipitation associated with discrete very low frequency emissions. J. Geophys. Res., **76**, 8445–8452.

ROSENBERG, T. J., MARTHINSEN, K., HOLTET, J. A., EGELAND, A. and CARPENTER, D. L. (1978): Evidence of the common origin of electron microbursts and VLF chorus. J. Geomagn. Geoelectr., **30**, 355–356.

SATO, M., MAEZAWA, K., FUKUNISHI, H. and SATO, N. (1983): Conjugacy of ELF emission spectra and powers. Mem. Natl Inst. Polar Res., Spec. Issue, **26**, 91–102.

SATO, N. and KOKUBUN, S. (1980): Interaction between ELF-VLF emissions and magnetic pulsations; Quasi-periodic ELF-VLF emissions associated with Pc 3–4 magnetic pulsations and their geomagnetic conjugacy. J. Geophys. Res., **85**, 101–113.

(Received April 23, 1984; Revised manuscript received May 14, 1984)